Ecology, 92(12), 2011, pp. 2202–2207

Estimation of population density by spatially explicit capture–recapture analysis of data from area searches

MURRAY G. EFFORD[1]

Zoology Department, University of Otago, P.O. Box 56, Dunedin, New Zealand

Abstract. The recent development of capture–recapture methods for estimating animal population density has focused on passive detection using devices such as traps or automatic cameras. Some species lend themselves more to active searching: a polygonal plot may be searched repeatedly and the locations of detected individuals recorded, or a plot may be searched just once and multiple cues (feces or other sign) identified as belonging to particular individuals. This report presents new likelihood-based spatially explicit capture–recapture (SECR) methods for such data. The methods are shown to be at least as robust in simulations as an equivalent Bayesian analysis, and to have negligible bias and near-nominal confidence interval coverage with parameter values from a lizard data set. It is recommended on the basis of simulation that plots for SECR should be at least as large as the home range of the target species. The R package "secr" may be used to fit the models. The likelihood-based implementation extends the spatially explicit analyses available for search data to include binary data (animal detected or not detected on each occasion) or count data (multiple detections per occasion) from multiple irregular polygons, with or without dependence among polygons. It is also shown how the method may be adapted for detections along a linear transect.

Key words: area search; Bayesian analysis; data augmentation; flat-tailed horned lizard; maximum likelihood; polygons; population density; spatially explicit capture–recapture; transects.

INTRODUCTION

Many animal species of conservation or economic importance are difficult to survey because they are mobile or cryptic, and only a fraction of the population is detected in any sample. Distance sampling and capture–recapture methods allow for incomplete detection, but in their simpler forms each method has limitations. Conventional distance sampling (Buckland et al. 2001) requires reliable determination of distances and does not allow for incomplete availability; closed-population capture–recapture does not allow for movement of animals between samples. Recently developed statistical methods overcome some of these limitations. Composite distance and capture–recapture methods address the problem of incomplete availability in distance sampling (e.g., Buckland et al. 2010). Spatially explicit capture–recapture (SECR) methods address the uncertain edge effects and spatially heterogeneous detection probability caused by movement in conventional animal trapping (Efford 2004, Borchers and Efford 2008). Spatial modeling of capture–recapture data requires attention to aspects of data collection that are of no import in nonspatial modeling. Broadly, different types of detector require different models. Efford et al. (2009*a*) distinguished traps that can catch several animals at once ("multi-catch traps") from single-catch traps and a further "proximity" detector type that records the presence of an animal at a point without restricting its movement. Efford et al. (2009*b*) discussed models for other types of detector that might be deployed at an array of points. For detector types other than single-catch traps, an integrated log-likelihood may be maximized numerically to fit the model and to estimate both detection parameters and population density (likelihood-based estimation appears to be intractable for single-catch traps and simulation methods are required; Efford 2004). Bayesian SECR implementations have been developed in parallel with likelihood-based approaches (Royle and Young 2008, Gardner et al. 2009, Royle et al. 2009), with two notable additions: Gardner et al. (2010) demonstrated an open-population model that allowed mortality during sampling, and Royle and Young (2008) dealt with the case that detections might be made anywhere within a polygon (in their case a square plot), rather than only at predetermined points. In this report, I show how data from searching plots ("polygon data") may be modeled in the likelihood SECR framework of Borchers and Efford (2008) and Efford et al. (2009*a*). Further methods for searches along linear transects are described in Appendix D.

Polygon data may be obtained by searching within a defined area directly for animals (given that some animals may be absent or not seen on a particular

Manuscript received 23 February 2011; revised 11 July 2011; accepted 25 July 2011. Corresponding Editor: B. D. Inouye.

[1] E-mail: murray.efford@otago.ac.nz

search) or indirectly for cues that can be identified to individual animals. Each search is a sampling "occasion" in the jargon of closed-population capture–recapture (Otis et al. 1978). Direct searches usually result in no more than one detection per animal per search ("binary data"), whereas multiple cues from an animal may be found on one search ("count data"). Models are presented here for both types of data. Physical cues such as feces or hair samples from different individuals can often be distinguished by their microsatellite DNA, and there is an increasing demand for statistical methods appropriate to these data. This has been met in part by the Bayesian data augmentation approach of Royle and Young (2008).

Whether ecologists use Bayesian or likelihood-based SECR methods will depend largely on availability and convenience, once certain performance criteria are met. Royle et al. (2009:3243) contended that "…Bayesian inferences… are valid regardless of the sample size" and "the practical validity of [maximum-likelihood] procedures cannot be asserted in most situations involving small samples." However, Marques et al. (2011) repeated the analyses and simulations of Royle and Young (2008), correcting some numerical errors, and identified bias and poor coverage of credible intervals for Bayesian estimates of density that they attributed in part to small samples. Marques et al. (2011) also speculated that with data for which Bayesian data augmentation performed poorly, one would also expect bias in the corresponding maximum-likelihood estimators.

However, likelihood-based methods are not without merit. For example, likelihood maximization is much faster than Markov chain Monte Carlo (MCMC) methods for fitting SECR models, and, within certain limits, is more flexible with respect to model selection and model averaging. How the performance of maximum-likelihood estimates of density compares with estimates from Bayesian data augmentation on the criteria of bias and confidence interval coverage is an empirical question that is answered here by Monte Carlo simulation. I first develop SECR methods for polygon data to fill this gap in the capture–recapture toolkit, and implement them in freely available software.

SECR Model for Data from Area Searches

I modify the general SECR model of Borchers and Efford (2008). Population density D is defined as the intensity of a Poisson spatial point process for home range centers, which are assumed to be fixed. The process may be homogeneous (D constant) or inhomogeneous (expected value $D(\mathbf{X};\boldsymbol{\phi})$ where $\boldsymbol{\phi}$ is a vector of parameters for a model relating density to location, $\mathbf{X}$, specified by a vector of coordinates x, y). The data comprise a set of detection histories $\boldsymbol{\omega}_i$ for the n observed individuals; the elements of $\boldsymbol{\omega}_i$ represent the detections of individual i on S successive occasions at a set of K detectors whose locations are known, along with ancillary data specific to each detection (e.g., sound intensity on a microphone array; Efford et al. 2009*b*). The probability of observing a particular $\boldsymbol{\omega}_i$ depends on a vector of detection parameters $\boldsymbol{\theta}$ and on $\mathbf{X}_i$, the unknown home range center of individual i; this unknown may be integrated out of the likelihood:

$$L(\boldsymbol{\theta},\boldsymbol{\phi}) \propto \Pr(n\,|\,\boldsymbol{\theta},\boldsymbol{\phi}) \times \prod_{i=1}^{n} \int \Pr(\boldsymbol{\omega}_i\,|\,\boldsymbol{\omega}_i > 0, \mathbf{X}, \boldsymbol{\theta}) f(\mathbf{X}\,|\,\boldsymbol{\omega}_i > 0, \boldsymbol{\theta}, \boldsymbol{\phi})\, d\mathbf{X}. \qquad (1)$$

Here $\boldsymbol{\omega}_i > 0$ indicates a non-null detection history (an animal detected at least once), and f is the probability density of centers, given that the animal was detected. Integration is over the real plane, or a subset of the plane representing potential habitat. Maximization of the likelihood provides estimates of $\boldsymbol{\phi}$ and $\boldsymbol{\theta}$. The likelihood is simpler when density is homogeneous, and in this case it is often sufficient to estimate $\boldsymbol{\theta}$ by maximizing the likelihood conditional on n and to compute a Horvitz-Thompson-like estimate of D. For details, the reader should consult Borchers and Efford (2008) and Efford et al. (2009*a*, *b*).

The preceding description is generic. For polygon data, each element of $\boldsymbol{\omega}_i$ comprises both the binary or integer number of detections of individual i on a particular occasion, and a vector of corresponding paired x-y coordinates equal in length to the number of detections, which may be zero. The development here is for binary data (maximum one detection per occasion); models are given in Appendix A for count data from other discrete distributions (Poisson, binomial), such as result from cue searches. Eq. 1 may be adapted for a particular detector type by substituting an appropriate model for the detection histories. For a detector at a point, such as a trap, detection probability is modeled as a decreasing function of the distance between the animal's home range center and the detector. For searches of a polygon, the probability of detection is a function of the quantitative overlap between the home range and the polygon (i.e., the instantaneous probability that an animal is within the polygon). We use p_{sk} to represent the probability of detecting a particular animal in polygon k on occasion s. Clearly p_{sk} depends on the location of the animal's home range relative to the polygon, on the size and shape of the home range, and on the efficiency of detection while the animal is within the polygon. We model the instantaneous location of an individual with a bivariate probability density function $h(\mathbf{u})$ where $\mathbf{u}$ represents a point in two dimensions, specified by a vector of coordinates (x, y); h is commonly circular bivariate normal, with a single scale parameter σ. Efficiency of detection is controlled by the parameter p_∞, which may be interpreted as the probability of detection when the home range is entirely within a search polygon. Unlike the one-dimensional functions used for point detectors (Borchers and Efford 2008), h must be integrated over

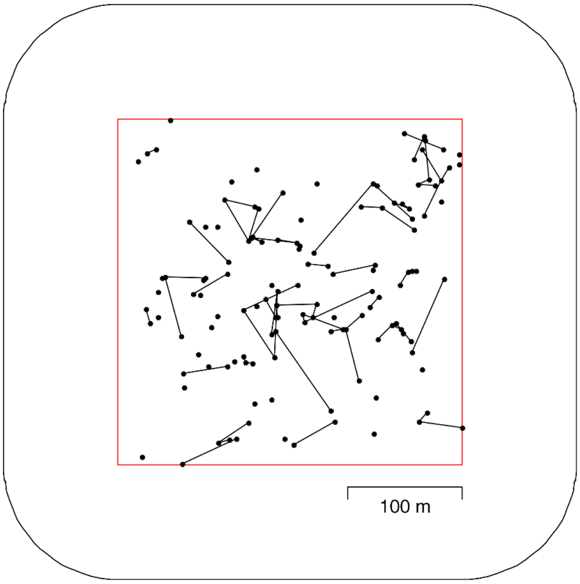

FIG. 1. Distribution of capture locations of flat-tailed horned lizards (*Phrynosoma mcallii*) within a square 300 × 300 m plot in southwestern Arizona, USA, on 14 search days. Lines join captures of the same individual. The outer boundary indicates an arbitrary 100-m buffer; home range centers were assumed to be distributed uniformly over the enclosed area.

the areal extent of each detector (indicated by κ) to obtain a probability of detection. Using $\boldsymbol{\theta}^-$ for the detection parameters other than p_∞, we have

$$p_{sk}(\mathbf{X}\,|\,\boldsymbol{\theta}) = p_\infty \int_{\kappa_k} h(\mathbf{u}\,|\,\mathbf{X};\boldsymbol{\theta}^-)\,d\mathbf{u}. \qquad (2)$$

These elements allow us to adapt Eq. 1 for polygon detectors. The first component of Eq. 1 has the same form as in the SECR models of Borchers and Efford (2008) and Efford et al. (2009*a*). Define $\lambda(\boldsymbol{\phi}, \boldsymbol{\theta}) = \int D(\mathbf{X}; \boldsymbol{\phi})p.(\mathbf{X}; \boldsymbol{\theta})\,\mathrm{d}\mathbf{X}$, where $p.(\mathbf{X})$ is the probability that an animal centered at $\mathbf{X}$ is detected at least once, given by $p.(\mathbf{X}\,|\,\boldsymbol{\theta}) = 1 - \prod_{s=1}^{S}\prod_{k=1}^{K}[1 - p_{sk}(\mathbf{X}\,|\,\boldsymbol{\theta})]$. Then, n is Poisson distributed with parameter λ, and $f(\mathbf{X}\,|\,\boldsymbol{\omega}_i > 0; \boldsymbol{\theta}, \boldsymbol{\phi}) = D(\mathbf{X}; \boldsymbol{\phi})p.(\mathbf{X}; \boldsymbol{\theta})/\lambda(\boldsymbol{\phi}, \boldsymbol{\theta})$. Alternatively, n may be modeled as a binomial draw from a fixed population of size N in an arbitrary area A (see Appendix A).

If detectors are independent, then the probability of observing a particular detection history, conditional on detection, is $\Pr(\boldsymbol{\omega}_i\,|\,\boldsymbol{\omega}_i > 0,\ \mathbf{X}; \boldsymbol{\theta}) = \prod_{s=1}^{S}\prod_{k=1}^{K} \Pr(\boldsymbol{\omega}_{iks}\,|\,\mathbf{X}; \boldsymbol{\theta})/p.(\mathbf{X}; \boldsymbol{\theta})$. For detectors that are not independent, see Appendix A). The unconditional probability has components for the probability of detection in each polygon and for the probability density of the observed location, conditional on detection in the polygon:

$$\Pr(\boldsymbol{\omega}_{iks}\,|\,\mathbf{X};\boldsymbol{\theta}) = \left[p_{sk}(\mathbf{X};\boldsymbol{\theta})h(\mathbf{u}\,|\,\mathbf{X};\boldsymbol{\theta}^-)\Big/\iint_{\kappa_k} h(\mathbf{u}\,|\,\mathbf{X};\boldsymbol{\theta}^-)\,d\mathbf{u}\right]^{\delta_{sk}} \times [1 - p_{sk}(\mathbf{X};\boldsymbol{\theta})]^{1-\delta_{sk}}$$

where $\delta_{sk} = 1$ if individual i was detected in polygon k on occasion s and $\delta_{sk} = 0$ otherwise.

IMPLEMENTATION

The model may be fitted numerically by maximizing the log likelihood as outlined by Borchers and Efford (2008) and Efford et al. (2009*a*) and implemented in the R package "secr" (Efford 2011). The integration in Eq. 1 is achieved by summing over a fine spatial grid, whereas the detection function (Eq. 2) is integrated by repeated one-dimensional Gaussian quadrature (Press et al. 1989). This is feasible and fast because h is circular and generally smooth and unimodal. The implementation is limited by the quadrature method to polygons that are convex, or concave only in one dimension, but otherwise allows for any shape or number of polygons, limited only by computer memory and speed.

The choice of shape for h is somewhat arbitrary. It is convenient to specify h as a radially symmetrical function g of the distance $r = |\mathbf{u} - \mathbf{X}|$, as used in point-detector implementations of SECR (e.g., Efford et al. 2009*a*). Suitable forms for $g(r)$ are halfnormal $g(r) = \exp[-r^2/(2\sigma^2)]$ or negative exponential $g(r) = \exp[-r/\sigma]$, corresponding, respectively, to Gaussian and Laplacian bivariate kernels. Other forms are available and may be preferred for particular data sets (Efford 2011). For h specified in this general way, normalization is necessary, but readily achieved in software by one-dimensional numerical integration

$$h(\mathbf{u}\,|\,\mathbf{X}) = \frac{g(r)}{2\pi \displaystyle\int_0^\infty rg(r)\,dr}.$$

Numerical estimates of the curvature of the likelihood surface at the MLE are used for the conventional asymptotic estimate of the variance–covariance matrix, from which symmetric Wald confidence limits ($\pm z_{\alpha/2}$SE) can be obtained for each parameter in the model. Here I used the logarithm of density for maximization and back-transformed the Wald limits to get an asymmetric interval for the MLE of density.

EXAMPLE

Royle and Young (2008) described a study in which a square 9-ha plot was searched for flat-tailed horned lizards (*Phrynosoma mcallii*) daily for 14 days. Lizards were marked and released at their point of capture. In total, 68 individuals were caught 134 times, distributed as shown in Fig. 1. Royle and Young (2008) fitted an uncorrelated Gaussian kernel for h, with separate scale parameters σ_1 and σ_2 for movements in the x- and y-dimensions. Their state space was a 25-ha square centered on the search area (J. A. Royle, *personal communication*). Deficiencies in the original implementation are corrected in Appendix B, where σ_1 and σ_2 are also combined in a single parameter σ (implicitly assuming no directional bias in movements). For likelihood-based analysis, a 64 × 64 grid was superim-

Table 1. Estimates of flat-tailed horned lizard (*Phrynosoma mcallii*) density and detection parameters using bivariate normal home range model fitted by (a) maximum likelihood or (b) Bayesian data augmentation.

	a) Likelihood-based analysis				b) Bayesian analysis		
			95% interval		Posterior		
Parameter	Estimate	SE′	Wald	Profile	Mean	SD	95% credible interval
Density					8.12	0.89	(6.56, 10.28)
Binomial *n*	8.03	0.90	(6.46, 9.99)	(6.47, 10.02)			
Poisson *n*	8.06	1.06	(6.23, 10.43)	(6.18, 10.37)			
p_∞	0.124	0.013	(0.100, 0.153)	(0.100, 0.152)	0.125	0.013	(0.099, 0.152)
σ	18.5	1.2	(16.3, 21.0)	(16.4, 21.1)	18.7	1.2	(16.5, 21.4)

Notes: The 95% intervals for the maximum-likelihood estimates (MLE) were either Wald intervals ($\pm z_{\alpha/2}$SE) back-transformed from the link scale (log, logit, and log for density, p_∞, and σ, respectively) or profile likelihood intervals. SE′ is the delta-method approximation to the standard error on the untransformed scale. Bayesian analysis was corrected from Royle and Young (2008) (see Appendix B). Detection parameters p_∞ (probability of detection when the home range is entirely within a search polygon) and σ (scale parameter) do not depend on the distribution assumed for number caught (*n*).

posed on the state space used by Royle and Young (2008), and the distribution of *n* was modeled as binomial to match their analysis; the fitted observation models were otherwise the same. R code for performing ML analyses with the package "secr" is given in Appendix C.

Maximum-likelihood estimates of horned lizard density and the detection parameters are shown in Table 1a. The MLE of density using a Gaussian kernel was slightly less than the mean of the posterior distribution estimated for essentially the same model by data augmentation and Markov chain Monte Carlo (MCMC), and its confidence interval was slightly shorter than the corresponding Bayesian credible interval (Table 1b). Numerical maximization of the likelihood took 83 seconds on a fast PC, compared to several hours for the corresponding Bayesian calculation. The model with a Laplace kernel fitted somewhat better (ΔAIC = 6.2), but the resulting density estimate was little different (8.06 ± 0.90 lizards/ha, mean ± SE); for consistency we focus on the model with a Gaussian kernel. Profile likelihood intervals were also obtained for the ML estimates, but they barely differed from the back-transformed Wald intervals (Table 1).

Simulations

Simulations (1000 replicates) were performed with the estimated parameter values from the horned lizard example to assess bias and confidence interval coverage. Data were generated under the Gaussian model and MLE obtained as described previously. Estimation failed for one simulated data set for unknown reasons. There was no evidence for positive or negative bias (estimated relative bias +0.4% ± 0.4%, mean ± SE). Coverage of the back-transformed 95% intervals was 93.1%. Although this is close to the nominal level, the 95% exact binomial interval for coverage (91.4–94.6%) does not include 95%.

Further simulations were performed to compare the performance of the likelihood-based method with that of Bayesian data augmentation as reported by Marques et al. (2011). Their scenarios comprised a sparse population (five levels from 0.234 to 0.781 individuals/ha) sampled by searching a square 1×1 km plot on five occasions (treating each of their units as 100 m); animals occupied circular normal home ranges with σ equal to 100 m, 200 m, or 400 m (see also Royle and Young 2008). The state space for both simulation and estimation was a square defined by a 3σ buffer around the plot. The detection parameter, here called p_∞, was held constant at 0.25. The average number of animals detected 1, 2, . . . , 5 times in 1000 simulations of each scenario closely matched (±1) the rounded values reported by Marques et al. (2011). The simulated data for some scenarios include very few recaptures, as stressed by Marques et al. (2011).

The maximum-likelihood estimator of density had substantially lower bias than the mean of the posterior distribution estimated using data augmentation, even when samples were very small (Table 2a). Marques et al. (2011) noted that the mode of the Bayesian posterior in their simulations was less biased than the mean. There is not a clear theoretical reason to choose the mode as a summary statistic, and empirically the mode was marginally less biased than the MLE for some scenarios ($\sigma = 1$) and much more biased than the MLE for others ($\sigma = 4$, $D \geq 0.469$). The coverage of 95% confidence intervals for the MLE was close to nominal levels for $\sigma = 1$ and $\sigma = 2$, whereas coverage of Bayesian credible intervals was impaired when $\sigma = 2$ (Table 2b). Coverage was poor for either method when $\sigma = 4$ and the plot was small relative to home range size. Plot area under these extreme scenarios was one-third that of the 95% home range, given that 95% of activity in a circular bivariate normal home range is expected to lie in a circle of area $18.8\sigma^2$ within 2.45σ of the center (Calhoun and Casby 1958). Other simulations (M. Efford, *unpublished data*) showed that the coverage of confidence intervals for density may be improved by using an elongated rectangular plot of the same area, intuitively because the longer plot spanned the home range diameter. However, this was not a complete solution, as there were fewer recaptures than with a square plot and estimates were still heavily biased.

TABLE 2. Performance of maximum-likelihood (ML) estimator for sparse capture–recapture data from polygon searches, compared to the Bayesian data-augmentation estimator of Royle and Young (2008) and Marques et al. (2011).

True density	a) Relative bias of density estimate as percentage									b) Interval coverage percentage					
	$\sigma = 1$			$\sigma = 2$			$\sigma = 4$			$\sigma = 1$		$\sigma = 2$		$\sigma = 4$	
	DA_{mn}	DA_{mo}	ML	DA_{mn}	DA_{mo}	ML	DA_{mn}	DA_{mo}	ML	DA	ML	DA	ML	DA	ML
0.234	21	5	8	30	10	17	51	31	35	95	95	89	96	90	76
0.352	12	1	3	24	9	8	60	47	25	98	97	92	95	83	79
0.469	10	1	3	20	7	6	58	46	17	97	96	89	95	76	82
0.586	6	0	2	17	8	4	62	54	10	93	96	92	96	72	82
0.781	6	1	1	17	10	4	46	36	7	97	95	90	95	74	87

Notes: Data augmentation (DA) results are presented for both the mean of the posterior distribution (DA_{mn}) and its mode (DA_{mo}); σ is the scale parameter of a circular bivariate normal activity distribution; see *Simulations* for other details. There were 1000 replicate simulations for ML and 100 replicates otherwise.

The effect of plot size relative to home range size on the performance of the likelihood-based density estimator was assessed in further simulations. These varied the number of square plots while holding the total search area and the expected number of repeat detections constant at 20 (by empirically adjusting overall density; Table 3). There was no evidence for deteriorating bias, precision, or confidence interval coverage until plots were less than $16\sigma^2$; marked bias and loss of precision and coverage were apparent at a plot area of $4\sigma^2$ (Table 3). Although these results are specific to the simulation scenario, they support a guideline that plots for SECR should not be much smaller than the home range of the animal. Precision will usually be inadequate for ecological inference in studies yielding fewer than 20 repeat detections (relative SE > 0.3). The suggested minimum plot size is conservative when sample sizes are larger.

DISCUSSION

Integration of areal searches into the maximum-likelihood framework for spatially explicit capture–recapture opens up new possibilities for ecological sampling. The horned lizard example used polygon searches to generate a binary daily capture data set similar to conventional trapping data sets, but with the addition of location-within-plot. If animals leave multiple, individually identifiable cues, there is no need for repeated searches because the model accepts within-occasion "recaptures" (Efford et al. 2009*b*). The methods are therefore useful for feces or hair samples identified by DNA from a single search. The present formulation allows multiple search polygons with irregular boundaries.

The maximum-likelihood estimators for polygon search data are compatible with the various extensions outlined by Borchers and Efford (2008) and implemented in the R package "secr." These include model selection and model averaging by AIC, estimation of range centers for observed individuals, pooling of parameters across multiple polygons, inclusion of covariates at various levels (time, individual, polygon), behavioral response to capture, and the fitting of trend models for density over space or time (Efford 2011). The model could be extended to allow uneven search effort within polygons, but this would require additional computation. In the present implementation, parts of a polygon with approximately homogeneous search intensity may be treated as separate polygons, and the intensity included in the model as a detector-level covariate.

TABLE 3. Effect of polygon size in relation to home range size on spatially explicit capture–recapture (SECR) estimates of density.

Plot area (σ^2)	No. plots	D (σ^{-2})	RB($\hat{D}$)	RSE($\hat{D}$)	Coverage (%)
1	64	131.9	0.47 (0.11)	224.46 (187.80)	70
2	32	82.2	0.20 (0.07)	1.43 (0.24)	72
4	16	58.5	0.12 (0.04)	0.62 (0.03)	86
8	8	47.6	0.02 (0.03)	0.39 (0.01)	92
16	4	42.8	0.02 (0.02)	0.30 (0.00)	96
32	2	40.4	0.02 (0.02)	0.27 (0.00)	96
64	1	39.1	−0.01 (0.02)	0.29 (0.00)	97

Notes: Simulated detection on five occasions with $p_\infty = 1.0$ and home range scale σ. Total search area was constant ($64\sigma^2$) but was subdivided into a varying number of isolated square plots of varying area (e.g., 95% home range, $18.8\sigma^2$). Population density (D) was varied as shown, keeping the expected number of repeat detections constant at 20. Performance of the SECR estimator $\hat{D}$ is summarized as relative bias (RB), relative standard error (RSE), and coverage of 95% nominal confidence intervals. There were 200 replicate simulations.

Searches are sometimes conducted along linear routes or "transects." If locations are recorded as distances along each transect, rather than perpendicular to the transect as in conventional distance sampling, the data may be analyzed with a linear variant of the present SECR methods as developed in Appendix D.

The assertion that Bayesian methods have greater "practical validity" (Royle et al. 2009) was not supported. Although likelihood theory establishes unbiasedness only for large samples, likelihood-based SECR estimators of density have been found to show negligible bias and near-nominal coverage of confidence intervals for ecologically realistic sample sizes (Efford et al. 2009*a*; this study). It appears likely that inadequate coverage of confidence intervals in some simulations was due to poor study design (i.e., largest dimension of plot less than diameter of home range) rather than to small samples. The similarity of maximum-likelihood estimates and corrected Bayesian estimates in the horned lizard example (Table 1) should increase confidence in the use of either method. However, the greater convenience and versatility of the likelihood implementation would appear to give it the edge.

ACKNOWLEDGMENTS

Andy Royle and Kevin Young generously provided the flat-tailed horned lizard data used in the example. Thanks to Len Thomas and Andy Royle for details of their analyses and for discussion. Suggestions by Tiago Marques, Deanna Dawson, and an anonymous reviewer substantially improved the manuscript.

LITERATURE CITED

Borchers, D. L., and M. G. Efford. 2008. Spatially explicit maximum likelihood methods for capture–recapture studies. Biometrics 64:377–385.

Buckland, S. T., D. R. Anderson, K. P. Burnham, J. L. Laake, D. L. Borchers, and L. Thomas. 2001. Introduction to distance sampling. Oxford University Press, Oxford, UK.

Buckland, S. T., J. Laake, and D. L. Borchers. 2010. Double-observer line transect methods: levels of independence. Biometrics 66:169–177.

Calhoun, J. B., and J. U. Casby. 1958. Calculation of home range and density of small mammals. Public Health Monograph 55. U.S. Government Printing Office, Washington, D.C., USA.

Efford, M. G. 2004. Density estimation in live-trapping studies. Oikos 106:598–610.

Efford, M. G. 2011. secr: spatially explicit capture–recapture models. R package version 2.1.0. ⟨http://cran.r-project.org/⟩

Efford, M. G., D. L. Borchers, and A. E. Byrom. 2009*a*. Density estimation by spatially explicit capture–recapture: likelihood-based methods. Pages 255–269 *in* D. L. Thomson, E. G. Cooch, and M. J. Conroy, editors. Modeling demographic processes in marked populations. Springer, New York, New York, USA.

Efford, M. G., D. K. Dawson, and D. L. Borchers. 2009*b*. Population density estimated from locations of individuals on a passive detector array. Ecology 90:2676–2682.

Gardner, B., J. Reppucci, M. Lucherini, and J. A. Royle. 2010. Spatially explicit inference for open populations: estimating demographic parameters from camera-trap studies. Ecology 91:3376–3383.

Gardner, B., J. A. Royle, and M. T. Wegan. 2009. Hierarchical models for estimating density from DNA mark–recapture studies. Ecology 90:1106–1115.

Marques, T. A., L. Thomas, and J. A. Royle. 2011. A hierarchical model for spatial capture–recapture data: comment. Ecology 92:526–528.

Otis, D. L., K. P. Burnham, G. C. White, and D. R. Anderson. 1978. Statistical inference from capture data on closed animal populations. Wildlife Monographs 62:1–135.

Press, W. H., B. P. Flannery, S. A. Teukolsky, and W. T. Vetterling. 1989. Numerical recipes in Pascal. Cambridge University Press, Cambridge, UK.

Royle, J. A., K. U. Karanth, A. M. Gopalaswamy, and N. S. Kumar. 2009. Bayesian inference in camera trapping studies for a class of spatial capture–recapture models. Ecology 90:3233–3244.

Royle, J. A., and K. V. Young. 2008. A hierarchical model for spatial capture–recapture data. Ecology 89:2281–2289.

APPENDIX A

Likelihood-based spatially explicit capture–recapture models for polygon searches (*Ecological Archives* E092-190-A1).

APPENDIX B

Revised analysis of horned lizard data set (Royle and Young 2008) (*Ecological Archives* E092-190-A2).

APPENDIX C

R code for likelihood-based analyses of horned lizard data and simulations (*Ecological Archives* E092-190-A3).

APPENDIX D

Likelihood-based spatially explicit capture–recapture models for linear searches (*Ecological Archives* E092-190-A4).